Original research paper

Population coherence and environmental impacts across spatial scales: a case study of Chinook salmon

Jan Ohlberger[1,*], Mark D. Scheuerell[2], and Daniel E. Schindler[1]

[1] School of Aquatic and Fishery Sciences, University of Washington, Seattle, WA 98195, USA

[2] Fish Ecology Division, Northwest Fisheries Science Center, National Marine Fisheries Service, National Oceanic and Atmospheric Administration, Seattle, WA 98112, USA

[*] Email: janohl@uw.edu (*corresponding author*)

ABSTRACT

A central problem in understanding how species respond to global change is in parsing the effects of local drivers of population dynamics from regional and global drivers that are shared among populations. Management and conservation efforts that typically focus on a particular population would benefit greatly from being able to separate the effects of environmental processes at local, regional and global scales. One way of addressing this challenge is to integrate data across multiple populations and use multivariate time series approaches to estimate shared and independent components of dynamics among neighboring populations. Here, we use a dataset of 15 populations of Chinook salmon (*Oncorhynchus tshawytscha*) covering a broad geographical range in the eastern North Pacific Ocean to show how Dynamic Factor Analysis (DFA) can be used to estimate temporal coherence in population dynamics and to detect environmental drivers across spatial scales. Our results show that productivity dynamics of Chinook salmon populations strongly covary at the regional scale, but to a lesser degree at larger spatial scales. The timing of river ice break-up in spring was identified as an important driver of regional productivity dynamics. In addition, broad-scale variability in population productivity was linked to the North Pacific Gyre Oscillation (NPGO), a dominant pattern of sea surface height variability. These broad-scale patterns in productivity dynamics may be associated with recent regime shifts in the Northeast Pacific Ocean. However, our results also demonstrate that populations within regions do not always respond consistently to the same environmental drivers, thus suggesting location-specific impacts. Overall, this study illustrates the use of DFA for quantifying the spatial and temporal complexity of multiple population responses to environmental change, thereby providing insights to processes that affect populations across large geographic areas, but that might be filtered by local habitat conditions.

Key words: coherence; environment; multivariate analysis; spatial scale; productivity dynamics.

INTRODUCTION

A central problem in understanding how species respond to global change is separating the local drivers that act independently on each population from the regional and global drivers that are shared among populations. Local environmental effects on population dynamics may result from changes in unique ecological conditions at a given location, or through filtering of regional environmental forcing through local habitat conditions (Hilborn et al. 2003, Rogers and Schindler 2011). Management and conservation focused on a particular population would benefit greatly from being able to isolate the effects of local conditions on population dynamics from those occurring at regional and global scales.

Population-level responses to environmental variation are integrated over space and time because the conditions experienced by an organism change due to ontogenetic development and shifts in habitat use. Migratory organisms are particularly prone to these effects (Runge et al. 2014, Jenni and Kéry 2003). For instance, in anadromous fishes, eggs and juveniles experience freshwater conditions specific to their natal stream, while adults are exposed to large-scale climate conditions in the ocean (Quinn 2005). In addition, life history, habitat variation, and limitations to dispersal interact to create spatial structure within species and populations (Levin 1992). Multiple populations of the same species thus experience environmental conditions that may or may not be shared, and may therefore respond differently to environmental change (Hilborn et al. 2003). Inferring environmental impacts and coherence in population responses from multiple population time series thus poses the challenge of accounting for the complex spatial, temporal, and organizational dependencies associated with ecological data, particularly when addressing issues related to climate change, harvesting, or species conservation.

One way of addressing this challenge is to use multivariate methods that reduce the dimensionality of the dataset under consideration to quantify dynamics that are shared among related time series. Although multivariate time series approaches have been widely used in finance for decades (Harvey 1989, Zuur et al. 2003a,b), their application to ecological time series is rare. Dynamic Factor Analysis (DFA) is a dimension reduction technique designed for multivariate time series analysis that has several advantages compared to ordination techniques such as Principal Component or Correspondence Analysis (Zuur et al. 2003a). DFA uses smooth trends, which are modeled as random walks and are shared among multiple observation time series, in order to detect spatial coherence between distinct populations or species. Further, covariates can easily be incorporated into the analysis, which allows characterizing the link between the populations and environmental factors as well as trends that are shared among populations but are not linked to known covariates. Finally, this framework can handle time series that vary in length or contain missing values, a challenge that ecologists commonly face when analyzing data that have been collected intermittently or by different research groups or management bodies.

In this study, we analyzed a data set of 15 populations of Chinook salmon (*Oncorhynchus tshawytscha*) whose spawning locations span nearly one million square kilometers across Alaska (USA) and the Yukon Territory (Canada). Chinook salmon is a highly valued species of Pacific salmon, and is important to commercial, recreational and subsistence fisheries throughout the North Pacific (Heard et al. 2007). In Alaska, many of the geographically distinct populations have experienced declines in productivity over the most recent decade (ADFG 2012, 2013), whereas other species of Pacific salmon in the region have not followed this trend (Ruggerone et al. 2010). In Western Alaska, recent declines in run abundance have resulted in closures of

commercial fisheries and restrictions in subsistence harvests (JTC 2013, Schindler et al. 2013). This broad-scale pattern of declines in abundance suggests common causality, e.g. due to large-scale climate variability. Here, we used DFA to characterize temporal and spatial patterns in the productivity of Chinook salmon populations across Alaskan rivers while controlling for impacts of freshwater and ocean conditions for which time series data exist. We subsequently examine the ability of the models to predict population productivity of Chinook salmon in these systems.

METHODS

Time series data

Chinook salmon is an anadromous fish inhabiting the Subarctic North Pacific Ocean and adjacent freshwater habitats. Adults return to fresh water in summer and fall to breed in their natal streams and rivers; they die shortly after spawning. Their eggs incubate overwinter and juveniles emerge in spring. Most Alaskan populations have a "stream-type" life history and typically spend at least a full year feeding in freshwater before migrating out to sea where they remain for 1-6 years before returning to spawn (Gilbert 1912, ADFG 2013). Chinook salmon are targeted by commercial, recreational and subsistence fisheries, and are caught as bycatch in other commercial fisheries (Stram and Ianelli 2014).

We used estimates of spawning escapement and subsequent recruits (catch + escapement) for 15 Chinook salmon populations with ocean entry locations throughout Alaska (Fig. 1), and calculated the natural logarithm of recruits per spawner as our index of population productivity (results when using residuals from a Ricker stock-recruitment fit as alternative productivity index are presented in the Appendix). The escapement and recruitment estimates derive from recent run reconstruction models (see Fleischmann et al. 2011, 2013), which were fit using a Bayesian state-space approach that simultaneously accounts for observation error and process noise. These

models were fit as follows: (1) recruitment is multiplied by estimated age-at-maturity parameters to predict age-specific abundances, which are fit to age composition data from the catch and escapement, (2) exploitation rates are estimated (e.g., based on mark-recapture data) to predict total harvest, which is then fit to observed harvest data (based on fishery trip reports and post-season surveys), and (3) escapement is predicted based on harvest and total abundance and fit to in-river abundance indices from air surveys or direct weir/tower counts.

Populations were clustered into three geographic areas based on the locations of the respective river mouths where smolts enter the ocean: Western Alaska (WAK), Southcentral Alaska (SCA), and Southeast Alaska (SEA). Western Alaska included the populations from the following rivers: Chena & Salcha (1986-2005), Goodnews (1981-2005), Kuskokwim (1976-2005), Nushagak (1976-2005), Unalakleet (1985-2005), and the Canadian Yukon (1982-2005). Southcentral Alaska included the populations from the following rivers: Anchor (1977-2005), Ayakulik (1976-2005), Deshka (1979-2005), Karluk (1976-2005), and Nelson (1976-2005). Because of its location, we considered including Nelson into the Western Alaska region, but our results suggest stronger coherence in productivity dynamics with the Southcentral Alaska populations. Southeast Alaska included the populations from the following rivers: Alsek (1976-2003), Situk (1982-2005), Stikine (1981-2005), and Taku (1976-2005).

Environmental indicators

We used a variety of indicators for environmental conditions experienced by Chinook salmon during the freshwater, estuarine and marine phases of their life cycle. Variables were lagged to correspond to the time period relative to the brood year when the environmental conditions that these indicators reflect were hypothesized to affect Chinook salmon survival. By using fixed lags, we assume that the life-history of the populations is characterized by a fixed age-structure

and that most individuals smolt at age 1 (e.g. a covariate with a time lag of 2 years is assumed to affect survival during the first year in the ocean). Because the model cannot handle missing data in the covariate time series (as opposed to missing data in the productivity time series data), we had to restrict our analysis to certain indicators, i.e. we eliminated some of the indicators that may be hypothesized to affect Chinook salmon productivity but had incomplete data. Data sources and lags considered for each indicator are provided in Table 2.

Environmental conditions considered for the freshwater phase were river ice break-up dates in spring (ICE), which has been linked to smolt migration timing (e.g. sockeye salmon, Hartman et al. 1967), and summer air temperature (TEMP) as a proxy for river temperature, which is known to influence the growth and survival of Chinook salmon fry in fresh water (McCullough 1999, Crozier et al. 2010). A complete time series of ice-break-up dates covering the entire study period was taken at Dawson on the upper Yukon River. This time series was used as a regional proxy for ice break-up dates in other rivers, which tend to be strongly correlated even over large distances (Jensen et al. 2007). For instance, ice break-up dates at Dawson and Bethel on the lower Kuskokwim River, which are about 1200 km apart, have a Pearson correlation of >0.7 (Bieniek et al. 2011). Regional time series of air temperature were taken at Faro, Yukon Territory (WAK), Anchorage (SCA), and Juneau (SEA). We used indicators for which long-term time series exist as our proxy for freshwater conditions across multiple populations, because the approach taken here cannot accommodate stock-specific indicators. Covariates are treated the same across populations for which shared trends are estimated, but the effect sizes of the covariates are population-specific.

Our ocean climate conditions were sea surface temperature (SST, winter/spring), sea level pressure (SLP, winter/spring), and a strong winds index (SWI) in the Bering Sea. Ocean

climate conditions may be especially important during the early marine phase of the salmon, i.e. during their first year at sea (Beamish and Mahnken 2001, Scheuerell et al. 2009, Wells et al. 2008, Burke et al. 2013). Accordingly, SSTs for the three regions were calculated by averaging temperatures within the areas bounded by 57-64°N and 157-169°W for WAK, 56-61°N and 146-157°W for SCA, and 54-60°N and 130-140°W for SEA, which were chosen to represent thermal conditions close to the stocks ocean-entry locations.

We included several indices that characterize climatic conditions across large spatial scales in the North Pacific and may thus integrate fish population responses across a wide geographical range. We used annual and winter indices of the Pacific Decadal Oscillation (PDO), a dominant pattern of temperature variability that has been linked to variability in Pacific salmon abundance (Mantua et al. 2002), and the North Pacific Gyre Oscillation (NPGO), a dominant pattern of sea surface height variability (Di Lorenzo et al. 2008). We also used the North Pacific Index (NPI) and the Arctic Oscillation (AO), which describe broad-scale patterns of sea level pressure variation.

We considered biotic indices of prey availability and competition, which also can be particularly important for salmon survival at sea (Beamish and Mahnken 2001). Specifically, we considered Kamchatka pink salmon (KAM) and walleye pollock biomass from the Bogoslof region in the Eastern Bering Sea (BOG). Older age-classes of Asian and North American salmon populations have overlapping distributions at sea and may compete for limited resources (Ruggerone et al. 2003), and Chinook salmon may prey upon or compete with walleye pollock (Davis et al. 2009). Finally, we used data on Russian Chinook catches (RUS) and the Bering Sea and Aleutian Islands (BSAI) Chinook bycatch, as these indices may reflect broad-scale changes in ecosystem dynamics that affect salmon survival. Changes in Russian catches may indicate

similar or inverse production dynamics of western and eastern Chinook populations in the North Pacific Ocean, whereas Chinook bycatch could either reflect changes in productivity, or negatively affect productivity by decreasing ocean survival in these populations.

Data analysis

Dynamic Factor Analysis (DFA) is a dimension reduction technique designed for multivariate time series analysis (Zuur et al. 2003a). The time series (**y**) are modeled as a linear combination of shared hidden trends (**x**), potential explanatory variables (**d**), and observation errors (**v**):

$$\mathbf{y}_t = \mathbf{Z}\,\mathbf{x}_t + \mathbf{D}\,\mathbf{d}_t + \mathbf{v}_t, \text{ where } \mathbf{v}_t \sim \text{MVN}(0, \mathbf{R})$$

Here, **Z** is a matrix of factor loadings on the hidden trends, and **D** is a matrix containing regression coefficients of the covariate effects. This formulation of the observation equation assumes that the time series have a mean of zero (otherwise a level parameter is required), and that the errors are normally distributed (MVN: multivariate normal) with mean zero and variance-covariance matrix **R**. The hidden trends (**x**) are modeled as random walk processes with a noise component (**w**):

$$\mathbf{x}_t = \mathbf{x}_{t-1} + \mathbf{w}_t \text{ , where } \mathbf{w}_t \sim \text{MVN}(0, \mathbf{I})$$

The process noise is assumed to be normally distributed with mean zero and variance-covariance matrix **I**, which is the identity matrix, i.e. the hidden trends are assumed to have a variance of 1 and no covariance structure. These trends are the information shared by the response variables that are not explained by the covariates. The initial state vector is set to a mean of zero and a diagonal variance-covariance matrix (**Λ**) with large variances:

$$\mathbf{x}_0 \sim \text{MVN}(\mathbf{0}, \mathbf{\Lambda})$$

Model parameters and states were estimated using the MARSS package (Holmes et al. 2012) in the programming environment **R** (R Development Core Team 2014).

We performed DFA analyses for Chinook salmon from the three regions: Western Alaska (6 populations), Southcentral Alaska (5 populations), and Southeast Alaska (4 populations). Populations within each region have ocean entry points in close geographic proximity (Fig. 1). In addition to the three regional models, we selected the most parsimonious model that included all 15 Alaskan Chinook salmon populations (indicators specific to the Bering Sea were not included). A maximum number of three shared trends was tested. We further allowed a maximum of three covariates in any single model to reduce the total number of models to be fit (i.e. we tested models without covariates and models with one, two, and three covariates). We tested the following error structures (**R** matrix): different variances and no covariance (*diagonal and unequal*), shared variance but no covariance (*diagonal and equal*), or shared variance and covariance (*equalvarcov*) between stocks. For the statewide model we also tested error structures with either shared variances and covariances by region, or shared variances but not covariances by region. Using the 1976-2005 brood years for our statewide and SCA analyses and the 1981-2005 brood years for our WAK and SEA analyses ensured that in any given year the model included data for at least three populations. However, we were able to include all datasets in the analysis, because the modeling approach smoothly handles missing data.

We used standard model selection based on the AICc to identify the explanatory model that contained the lowest number of common trends without suffering from much information loss, included the most relevant explanatory variables, and used the most parsimonious form of the variance-covariance matrix. The model with the lowest AICc value was selected as the best model, and models with a ΔAICc of less than 2 were considered competitive models with similar support (Burnham and Anderson 2002). We subsequently performed a retrospective analysis to evaluate the ability of the selected model to accurately forecast Chinook salmon population

productivity in each of the three regions. To accomplish this, we computed one-step-ahead forecasts from the DFA model and used the predictions for each year to calculate an overall forecast error, which was defined as the square root of the mean squared prediction error (RMSE). Using this metric of predictive ability, we compared the selected models including covariates, i.e. the model with the greatest support according to the AICc model selection, to (1) trend-only DFA models without covariates, (2) models that in any given year use the previous observation as predicted value, and (3) models that produce predictions by randomly drawing from a normal distribution with a mean and variance derived from the respective time series.

RESULTS

The statewide model with the greatest data support estimated two common trends in recruitment dynamics among the 15 Chinook populations (Fig. 2). The first trend was characterized by a period of above-average productivity around 1981-1992 and a moderate decline towards the end of the time series. A steep drop in productivity during the early 2000s dominated the second trend. Overall these trends combined to produce particularly low productivity during the most recent decade. The population loadings on these trends tended to be clustered by region: WAK populations showed mostly positive loadings on the first trend and SCA populations showed strong positive loadings on the second trend, while SEA populations were associated with both trends. The best model included the winter NPGO as a global environmental indicator of Chinook salmon productivity across Alaska that explained additional variation beyond the two trends described above. The NPGO in year 2, i.e. two years after the brood year, showed mostly positive and some negative associations with population productivity, and the effect was significant for some of the stocks (Fig. 3). In particular, Chinook salmon returning to the Kuskokwim, Yukon, Anchor, Stikine and Taku rivers were all positively correlated with the

NPGO. The best model included an error structure of variances and covariances that were identical within regions but different between regions. The second and third most parsimonious model included three common trends. However, all alternative models tested in the statewide analysis had a ΔAICc>2 (Appendix, Table A1).

The regional models with the greatest data support had only a single common trend within each region (Fig. 4). Populations consistently showed positive loadings on the detected trends, suggesting that population productivity followed similar temporal dynamics within regions. In line with the statewide model, these models suggest declining productivity towards the end of the time series, beginning with the 2000 brood year, approximately. Both the shared trends and selected indicators differed by region, suggesting less coherent dynamics among regions (Figs. 4 and 5).

Higher productivity in WAK populations was associated with earlier ice break-up in year 2, lower Russian Chinook catches in year 3, and a positive winter NPGO index in year 2. The SCA model included BSAI Chinook bycatch and BOG pollock biomass in year 2, and Russian Chinook catches in year 3, however, these indicators showed inconsistent associations with Chinook population productivity in the SCA region.

Higher productivity of SEA populations was weakly associated with increased Russian Chinook catches in year 3, and showed weak associations to the timing of ice break-up in year 1. In the case of WAK and SEA several alternative models had a ΔAICc<2, suggesting that other indicators such as the PDO are linked to population productivity in these regions (Appendix, Tables A2-A4). The observation error structure indicated that populations share the same variance by region and that models with or without a uniform covariance structure perform

similarly well. Overall, model fits captured both the long-term trends and interannual variability of the data (Fig. 6, see also Fig. A1).

Using a different regional clustering with the Nelson River population as part of a larger Western Alaska region produced slightly different results. This alternative DFA selected the same covariates for the most parsimonious WAK models, but instead estimated two shared trends, which suggested less coherent dynamics among WAK populations when Nelson was included in the region. The SCA model without Nelson estimated one shared trend and selected similar covariates (Appendix, Tables A5-A6).

Compared to models without covariates, the selected regional models had higher predictive power when performing one-year ahead forecasts of population productivity. The covariate models had the lowest forecast errors, followed by trend-only models without covariates and models that used the previous observation as predicted value (Fig. 7). However, the relative performance of the different models varied by population and region. As expected, models using the previous observation as predicted value produced weak forecasts in populations with volatile productivity dynamics, but performed reasonably well in populations characterized by strong autocorrelation in the time series. Including covariates into the regional models reduced population-specific forecast errors by an average of 19% across all 15 populations. The strongest effect was found for Western Alaska populations with an average reduction in forecast error of 29% across populations.

DISCUSSION

We found strong support for temporal synchrony in Chinook salmon productivity dynamics within regions and some support for synchronous dynamics at larger spatial scales across Alaska (i.e., among regions, Fig. 1). The regional models had only one common trend in each of the

three regions (Fig. 4), and populations showed regional clustering in the statewide analysis (Fig. 2). The estimated trends demonstrate that productivity of Alaskan Chinook salmon has generally declined during the most recent decade, starting around 2000. Our results further suggest that the timing of river ice break-up (an indicator of regional spring warming) is a potentially important factor determining population productivity in Western Alaska, and that productivity dynamics of Chinook salmon across Alaska are linked to the NPGO index. However, the results also show that populations within regions do not respond consistently to the same environmental drivers, suggesting that environmental effects on recruitment are regulated at local scales. Our findings further indicate that broad-scale changes in Chinook salmon productivity may be linked to recent regime shifts in the North Pacific Ocean. The climate of the North Pacific experienced regime shifts in 1977 and 1989 (Hare and Mantua 2000). The statewide model trends show increased productivity to above-average levels shortly after 1977 and a decline shortly after 1989 (Fig. 2). Declines in productivity in Western Alaskan Chinook salmon appeared to be especially linked to the 1989 regime shift (Fig. 4).

The finding that Chinook salmon productivity dynamics covary at the regional scale is consistent with previous studies on other species of Pacific salmon showing that correlations in survival indices of pink (*O. gorbuscha*), chum (*O. keta*), and sockeye (*O. nerka*) salmon tend to be higher at smaller distances (Mueter et al. 2002, Peterman et al. 1998, Pyper et al. 2001, Sharma et al. 2013, Stachura et al. 2014). For instance, Peterman and Dorner (2012) showed that productivity of sockeye salmon from Washington to Southeast Alaska has declined markedly since the late 1990s, while productivity of central and western Alaskan populations has increased or varied only slightly over the same time period, suggesting different productivity dynamics between regions.

While our analysis identified regional covariability in Chinook salmon productivity, it also indicated some degree of variation in the population-specific effects of environmental drivers. This is in line with recent studies that have demonstrated intraspecific variation in population responses to the same regional climate variables in Pacific salmon (Hilborn et al. 2003, Schindler et al. 2010, Braun et al. 2015). For instance, Braun et al. (2015) showed that ocean environmental conditions (e.g. offshore temperature) had contrasting effects on the survival of Chinook salmon populations in the Fraser River (Canada) that differed in life history. Population-specific responses may also reflect geographic variation in the relationship between broad-scale climate indices and local climate conditions, for instance via differences in habitat characteristics (van de Pol et al. 2013).

The North Pacific Gyre Oscillation (NPGO) was associated with Chinook salmon productivity dynamics at large spatial scales (Fig. 3), indicating that the NPGO is more closely linked to variability in Chinook salmon dynamics than other broad-scale climate indices. The NPGO has previously been linked to the productivity of krill and higher trophic levels in the Northeast Pacific (Sydeman et al. 2013). Our results complement a recent study on hatchery-reared Chinook salmon indicating that the NPGO is an important driver of variability in Chinook salmon populations along the West Coast, from California to Southeast Alaska (Kilduff et al. 2015). Specifically, it was shown that variability in ocean conditions, as reflected by the NPGO, acts to synchronize survival rates of Chinook and coho salmon across a broad geographic range.

At the regional scale, river ice break-up dates had significant effects on Chinook salmon productivity. Variability in river ice break-up dates reflects general changes in climate conditions and has been linked to larger climate indices such as the PDO (Schindler et al. 2005, Schindler and Rogers 2009). Because stream-type Chinook spend one winter in freshwater, conditions such

as river ice break-up that affect growth potential may affect survival during subsequent winters. Furthermore, ice break-up date may affect ocean survival through changes in the timing of smolt migration (Scheuerell et al. 2009, Satterthwaite et al. 2014). Thus, earlier ice break-up may affect productivity in Alaskan salmon populations through advanced outmigration of smolts or earlier warming of rivers leading to better growth conditions. Chinook populations at high latitudes may therefore benefit from changes in freshwater conditions due to a warming climate. In contrast, previous studies have suggested that Chinook salmon might be particularly vulnerable to future changes in ocean conditions due to climate change (Abdul-Aziz et al. 2011, Sharma et al. 2013).

Forecast errors were used as a measure of predictive power to evaluate the degree to which environmental indicators could improve the models' ability to produce one-year-ahead projections of population productivity, as compared to random walk only and simple autoregressive models. Including the selected indicators generally improved the predictive ability of the models (Fig. 7). This was particularly evident for populations from Western Alaska. Consequently, obtaining information on environmental variables that are known to affect Chinook salmon at specific life-stages, for instance the timing of river ice break-up in the year that salmon smolts migrate to the ocean, can improve forecasts of population productivity.

The models presented here do not account for density dependence in the spawner-recruit relationship, because we used ln(R/S) time series as our index of population productivity. However, we also ran our analyses using the residuals of a Ricker stock-recruitment fit to account for density dependence effects. The results obtained using this alternative index of population productivity are largely in line with the findings reported for ln(R/S) time series (Appendix, Table A7, Figs. A2 and A3). The statewide model had the same number of trends, and included the NPGO index with similar estimated effect sizes, though also included the BSAI

Chinook bycatch as additional indicator (Fig. A2). The regional models had either one or two trends and tended to select similar but fewer indicators in the top models (Table A7, Fig. A3). The direction and strength of the covariate effects were mostly consistent (Figs. 5 and A3), e.g. the strongest, most significant effects were found for river ice break-up in Western Alaska.

While the dominant life-history pattern across the study populations can be classified as 'stream-type', i.e. the majority of individuals spend a full year in freshwater habitats, it should be noted that the Situk river population in Southeast Alaska exhibits a distinct life-history in that most individuals migrate to sea as sub-yearling smolts (McPherson et al. 2003). This may have limited our ability to identify important indicators of productivity dynamics in this region, because for this population indicators were tested for effects during the second (not first) year of marine life. Interestingly, the timing of river ice break-up in the first year was found to be significant for this population, which is in line with the expectation that ice break-up in the year of outmigration is an important driver of Chinook salmon productivity (Fig. 5). Another potential limitation of our approach is that the life-history of the populations may have changed over time. Hence, changes in the proportion of the dominant age-class that migrates out to the ocean over the time period studied here cannot be ruled out.

Finally, other environmental drivers that were not included in this study may affect growth and survival of Chinook salmon, specifically trophic interactions that could not be accounted due to a lack of long-term time series data. For instance, a potentially important factor is the prevalence of *Ichthyophonus*, a parasite that has recently increased in abundance and that may affect the spawning success of Alaskan Chinook salmon, such as has been hypothesized for the Yukon River population (Kocan et al. 2003).

In conclusion, our findings suggest that productivity dynamics of Chinook salmon populations strongly covary within regions and to some extend across large spatial scales. The estimated temporal trends further suggest that Chinook salmon productivity in Alaskan rivers has declined markedly in the early 2000s. Finally, this study illustrates the use of Dynamic Factor Analysis for quantifying the spatial and temporal complexity of multiple population responses to changes in environmental conditions. This approach formally extracts trends that are common to populations but that are not explained by known covariates and therefore will provide insights to broad-scale processes that affect population dynamics across large regions.

ACKNOWLEDGEMENTS

We thank S. Fleischman and M. Catalano for providing run reconstructions of spawning escapement and recruitment for the populations used in this analysis. We also thank K. Myers and M. Bradford who provided additional time series data on environmental indicators, and M. Stachura for helpful discussions. Input from S. Fleishman, R. Clark, E. Volk, and J. Linderman from the Alaska Department of Fish and Game was invaluable to this project. This work was funded by the Arctic-Yukon-Kuskokwim Sustainable Salmon Initiative, and we thank J. Spaeder for his insights on this effort.

LITERATURE CITED

Abdul-Aziz, O. I., N. J. Mantua, K. W. Myers, and M. Bradford. 2011. Potential climate change impacts on thermal habitats of Pacific salmon (*Oncorhynchus spp*.) in the North Pacific Ocean and adjacent seas. Canadian Journal of Fisheries and Aquatic Sciences 68:1660–1680.

ADFG 2012. Alaska Chinook salmon knowledge gaps and needs. Alaska Department of Fish and Game. Anchorage, AK.

ADFG Chinook Salmon Research Team. 2013. *Chinook salmon stock assessment and research plan, 2013*. Alaska Department of Fish and Game, Special Publ. No. 13-01, Anchorage, AK.

Beamish, R. J., and C. Mahnken. 2001. A critical size and period hypothesis to explain natural regulation of salmon abundance and the linkage to climate and climate change. Progress in Oceanography 49:423–437.

Bieniek, P. A., U. S. Bhatt, L. A. Rundquist, S. D. Lindsey, X. Zhang, and R. L. Thoman. 2011. Large-scale climate controls of interior Alaska river ice breakup. Journal of Climate 24:286–297.

Braun, D. C., J. W. Moore, J. Candy, and R. E. Bailey. 2015. Population diversity in salmon: linkages among response, genetic and life history diversity. Ecography. [doi 10.1111/ecog.01102]

Burke, B. J., W. T. Peterson, B. R. Beckman, C. Morgan, E. A. Daly, and M. Litz. 2013. Multivariate Models of Adult Pacific Salmon Returns. PLoS ONE 8:e54134.

Crozier, L. G., R. W. Zabel, E. E. Hockersmith, and S. Achord. 2010. Interacting effects of density and temperature on body size in multiple populations of Chinook salmon. Journal of Animal Ecology 79:342–349.

Davis, N. D., K. W. Myers, and W. J. Fournier. 2009. Winter food habits of Chinook salmon in the eastern Bering Sea. North Pacific Anadromous Fish Commission Technical Report 5:243–253.

Di Lorenzo, E., N. et al. 2008. North Pacific Gyre Oscillation links ocean climate and ecosystem change. Geophysical Research Letters 35:L08607.

Fleischman, S. J., M. J. Catalano, R. A. Clark, D. R. Bernard, and Y. Chen. 2013. An age-structured state-space stock–recruit model for Pacific salmon (*Oncorhynchus spp*.). Canadian Journal of Fisheries and Aquatic Sciences 70:401–414.

Fleischman, S. J., Der Hovanisian, J. A., and McPherson, S. A. 2011. Escapement goals for Chinook salmon in the Blossom and Keta Rivers. Fishery Manuscript No. 11-05. Alaska Department of Fish and Game, Anchorage, AK.

Gilbert, C. H. 1912. Age at maturity of Pacific Coast salmon of the Genus *Oncorhynchus*. Bulletin of the United States Bureau of Fisheries 32:1–22.

Hare, S. R., and N. J. Mantua. 2000. Empirical evidence for North Pacific regime shifts in 1977 and 1989. Progress in Oceanography 47:103–145.

Hartman, W. L., W. R. Heard, and B. Drucker. 1967. Migratory behavior of sockeye salmon fry and smolts. Journal of the Fisheries Research Board of Canada 24:2069–2099.

Harvey, A.C. 1989. Forecasting, structural time series models and the Kalman filter. Cambridge University Press, Cambridge.

Heard, W. R., E. Shevlyakov, O. V. Zikunova, and R. E. McNicol. 2007. Chinook salmon – trends in abundance and biological characteristics. North Pacific Anadromous Fish Commission Bulletin 4:77–91.

Hilborn, R., T. P. Quinn, D. E. Schindler, and D. E. Rogers. 2003. Biocomplexity and fisheries sustainability. Proceedings of the National Academy of Sciences of the United States of America 100:6564–6568.

Holmes, E. E., E. J. Ward, and K. Wills. 2012. MARSS: Multivariate autoregressive state-space models for analyzing time-series data. The R Journal 4:11–19.

Jenni, L., and M. Kery. 2003. Timing of autumn bird migration under climate change: advances in long-distance migrants, delays in short-distance migrants. Proceedings of the Royal Society B: Biological Sciences 270:1467–1471.

Jensen, O. P., B. J. Benson, J. J. Magnuson, V. M. Card, M. N. Futter, P. A. Soranno, and K. M. Stewart. 2007. Spatial analysis of ice phenology trends across the Laurentian Great Lakes region during a recent warming period. Limnology and Oceanography 52:2013–2026.

JTC (The United States and Canada Yukon River Joint Technical Committee). 2013. Yukon River salmon 2012 season summary and 2013 season outlook. Alaska Department of Fish and Game, Division of Commercial Fisheries, Reg. Info. Rep. 3A13-01. Anchorage, AK.

Kilduff, D. P., E. Di Lorenzo, L. W. Botsford, and S. L. H. Teo. 2015. Changing central Pacific El Niños reduce stability of North American salmon survival rates. Proceedings of the National Academy of Sciences of the United States of America:201503190–5.

Kocan, R., P. Hershberger and J. Winton. 2003. Effects of *Ichthyophonus* on Survival and Reproductive Success of Yukon River Chinook Salmon. Federal Subsistence Fishery Monitoring Program, Final Project Report No. FIS 01-200. U. S. Fish and Wildlife Service, Office of Subsistence Management, Fishery Information Services Division, Anchorage, Alaska.

Levin, S. 1992. The problem of pattern and scale in ecology. Ecology 73:1943–1967.

McPherson, S., D. Bernard, J. H. Clark, K. Pahlke, E. Jones, J. Der Hovanisian, J. Weller, and R. Ericksen. 2003. Stock status and escapement goals for Chinook salmon stocks in

Southeast Alaska. Alaska Department of Fish and Game, Special Publication No. 03-01, Anchorage, AK.

Mantua, N. J., and S. R. Hare. 2002. The Pacific decadal oscillation. Journal of Oceanography 58:35–44.

McCullough, D. A. 1999. A review and synthesis of effects of alterations to the water temperature regime on freshwater life stages of salmonids, with special reference to Chinook salmon. USEPA Report.

Mueter, F. J., D. M. Ware, and R. M. Peterman. 2002. Spatial correlation patterns in coastal environmental variables and survival rates of salmon in the north-east Pacific Ocean. Fisheries Oceanography 11:205–218.

Peterman, R. M., and B. Dorner. 2012. A widespread decrease in productivity of sockeye salmon (*Oncorhynchus nerka*) populations in western North America. Canadian Journal of Fisheries and Aquatic Sciences 69:1255–1260.

Peterman, R. M., B. J. Pyper, M. F. Lapointe, M. D. Adkison, and C. J. Walters. 1998. Patterns of covariation in survival rates of British Columbian and Alaskan sockeye salmon (*Oncorhynchus nerka*) stocks. Canadian Journal of Fisheries and Aquatic Sciences 55:2503–2517.

Pyper, B. J., F. J. Mueter, R. M. Peterman, D. J. Blackbourn, and C. C. Wood. 2001. Spatial covariation in survival rates of Northeast Pacific pink salmon (*Oncorhynchus gorbuscha*). Canadian Journal of Fisheries and Aquatic Sciences 58:1501–1515.

Quinn, T. P. 2005. The Behavior and Ecology of Pacific Salmon and Trout. University of Washington Press, Seattle, WA.

R Development Core Team. 2014. R: A language and environment for statistical computing. Third edition. R Foundation for Statistical Computing, Vienna, Austria.

Rogers, L. A., and D. E. Schindler. 2011. Scale and the detection of climatic influences on the productivity of salmon populations. Global Change Biology 17: 2546–2558.

Ruggerone, G. T., M. Zimmermann, K. W. Myers, J. L. Nielsen, and D. E. Rogers. 2003. Competition between Asian pink salmon (*Oncorhynchus gorbuscha*) and Alaskan sockeye salmon (*O. nerka*) in the North Pacific Ocean. Fisheries Oceanography 12:209–219.

Ruggerone, G. T., R. M. Peterman, B. Dorner, and K. W. Myers. 2010. Magnitude and trends in abundance of hatchery and wild pink salmon, chum salmon, and sockeye salmon in the North Pacific Ocean. Marine and Coastal Fisheries 2:306–328.

Runge, C. A., T. G. Martin, H. P. Possingham, S. G. Willis, and R. A. Fuller. 2014. Conserving mobile species. Frontiers in Ecology and the Environment 12:395–402.

Scheuerell, M. D., R. W. Zabel, and B. P. Sandford. 2009. Relating juvenile migration timing and survival to adulthood in two species of threatened Pacific salmon (*Oncorhynchus spp.*). Journal of Applied Ecology 46:983–990.

Schindler, D. E., and L. A. Rogers. 2009. Responses of Pacific salmon populations to climate variation in freshwater ecosystems. Pages 1127–1142 *in* C. C. Krueger and C. E. Zimmerman, editors. Pacific Salmon - Ecology and Management of Western Alaska's Populations. American Fisheries Society. Bethesda, MA.

Schindler, D. E., et al. 2013. Arctic-Yukon-Kuskokwim Chinook salmon research action plan. AYK Sustainable Salmon Initiative. Anchorage, AK.

Schindler, D. E., D. E. Rogers, M. D. Scheuerell, and C. A. Abrey. 2005. Effects of changing climate on zooplankton and juvenile sockeye salmon growth in southwestern Alaska. Ecology 86:198–209.

Schindler, D. E., R. Hilborn, B. Chasco, C. P. Boatright, T. P. Quinn, L. A. Rogers, and M. S. Webster. 2010. Population diversity and the portfolio effect in an exploited species. Nature 465:609–613.

Sharma, R., L. A. Vélez-Espino, A. C. Wertheimer, N. Mantua, and R. C. Francis. 2013. Relating spatial and temporal scales of climate and ocean variability to survival of Pacific Northwest Chinook salmon (*Oncorhynchus tshawytscha*). Fisheries Oceanography 22:14–31.

Stachura, M. M., N. J. Mantua, and M. D. Scheuerell. 2014. Oceanographic influences on patterns in North Pacific salmon abundance. Canadian Journal of Fisheries and Aquatic Sciences 71:226–235.

Stram, D. L., and J. N. Ianelli. 2014. Evaluating the efficacy of salmon bycatch measures using fishery-dependent data. ICES Journal of Marine Science:1–8.

Sydeman, W. J., J. A. Santora, S. A. Thompson, B. Marinovic, and E. D. Lorenzo. 2013. Increasing variance in North Pacific climate relates to unprecedented ecosystem variability off California. Global Change Biology 19:1662–1675.

van de Pol, M., et al. 2013. Problems with using large-scale oceanic climate indices to compare climatic sensitivities across populations and species. Ecography 36:249–255.

Wells, B. K., C. B. Grimes, J. G. Sneva, S. McPherson, and J. B. Waldvogel. 2008. Relationships between oceanic conditions and growth of Chinook salmon (*Oncorhynchus*

tshawytscha) from California, Washington, and Alaska, USA. Fisheries Oceanography 17:101–125.

Zuur, A. F., I. D. Tuck, and N. Bailey. 2003a. Dynamic factor analysis to estimate common trends in fisheries time series. Canadian Journal of Fisheries and Aquatic Sciences 60:542–552.

Zuur, A. F., R. J. Fryer, I. T. Jolliffe, R. Dekker, and J. J. Beukema. 2003b. Estimating common trends in multivariate time series using dynamic factor analysis. Environmetrics 14:665–685.

Table 1. Chinook salmon escapement and recruitment time series used in the DFA. Given are years for which data were included and the average recruitment and escapement across years.

Stock	Years	Average recruitment	Average escapement
Chena & Salcha	1986-2005	30311	17226
Goodnews	1981-2005	9297	6357
Kuskokwim	1976-2005	248083	160585
Nushagak	1976-2005	224748	146074
Unalakleet	1985-2005	8919	3455
Yukon (Canadian)	1982-2005	122431	52085
Anchor	1977-2005	10988	10081
Ayakulik	1976-2005	13024	10691
Deshka	1979-2005	29534	25024
Karluk	1976-2005	9704	8789
Nelson	1976-2005	8176	4758
Alsek	1976-2003	8873	9115
Situk	1982-2005	3591	1522
Stikine	1981-2005	44499	32525
Taku	1976-2005	58096	48510

Table 2. Environmental indicators used in the DFA. Indicators were hypothesized to affect Chinook salmon at specific ages, and were lagged by the appropriate year, relative to brood year.

		Year					
Indicator	Acronym	1	2	3	4	5	Source
Air temperature on land	TEMP	X	X				1,2
Ice-out dates	ICE	X	X				3
Sea level pressure	SLP		X				2
Sea-surface temperature	SST		X				2
Strong winds index	SWI		X				2
Arctic Oscillation	AO		X				2
Pacific Decadal Oscillation	PDO		X				2
North Pacific Index	NPI		X				2
North Pacific Gyre Oscillation	NPGO		X				4
Bogoslof region pollock biomass	BOG		X				5
Russian Chinook catch	RUS			X	X	X	5
Kamchatka pink abundance	KAM			X			6
BSAI Chinook bycatch	BSAI		X	X	X		6

Sources are: 1, M. Bradford, personal communication; 2, Bering Climate, NOAA (http://www.beringclimate.noaa.gov); 3, Alaska-Pacific River Forecast Center, NOAA (http://aprfc.arh.noaa.gov); 4, Emanuele Di Lorenzo (http://www.o3d.org/npgo); 5, Kate Myers, University of Washington, pers. comm.; 6, North Pacific Anadromous Fish Commission (http://www.npafc.org).

FIGURE CAPTIONS

Fig. 1: Map of Alaska with Chinook salmon productivity time series by region. Chinook salmon populations were clustered according to their ocean entry locations into the following three regions: Western Alaska (WAK), Southcentral Alaska (SCA), and Southeast Alaska (SEA). Productivity time series were demeaned and standardized.

Fig. 2: Trends and loadings of the statewide model. Shown are common trends and population-specific loadings on these trends for the statewide model that included all 15 Chinook populations.

Fig. 3: Covariate effects of the statewide model. Shown are maximum likelihood estimates and 95% confidence intervals for the NPGO effect, which was the only indicator that was included into the most parsimonious model. CIs were calculated based on the hessian approach by re-fitting the DFA using the maximum likelihood estimates produced by the original model that allowed for an error structure of different variances and covariances by region.

Fig. 4: Trends and loadings of the regional models. Shown are common trends and population-specific loadings on these trends for each of the regions: WAK (top/blue), SCA (center/green), and SEA (bottom/purple).

Fig. 5: Covariate effects of the regional DFA models. Shown are maximum likelihood estimates and 95% confidence intervals for covariates included into the most parsimonious model for each region: WAK (left/blue), SCA (center/green), SEA (right/purple). The WAK and SCA models included three indicators, and the SEA model included two indicators (ICE: river

ice break-up, NPGO: North Pacific Gyre Oscillation, RUS: Russian Chinook catches, BSAI: Bering Sea and Aleutian Islands Chinook bycatch, BOG: Bogoslof region pollock biomass).

Fig. 6: Fits of the regional DFA models. Shown are model fits to productivity time series of all Chinook populations by region: WAK (left/blue), SCA (center/green), and SEA (right/purple).

Fig. 7: Comparison of model predictive ability. Shown are forecast errors for each population of the selected regional models including covariates (covar) in comparison with trend-only models (trend), models that in each year use the previous observation as predicted value (prev), and models that produce predictions by randomly drawing from a normal distribution with a mean and variance derived from the respective time series (rand). Circles and lines for the random forecast model represent median values and 95% confidence intervals based on 10,000 bootstraps. The selected covariate models tended to have the lowest forecast errors (square root of the mean squared prediction error) and thus the best predictive power.

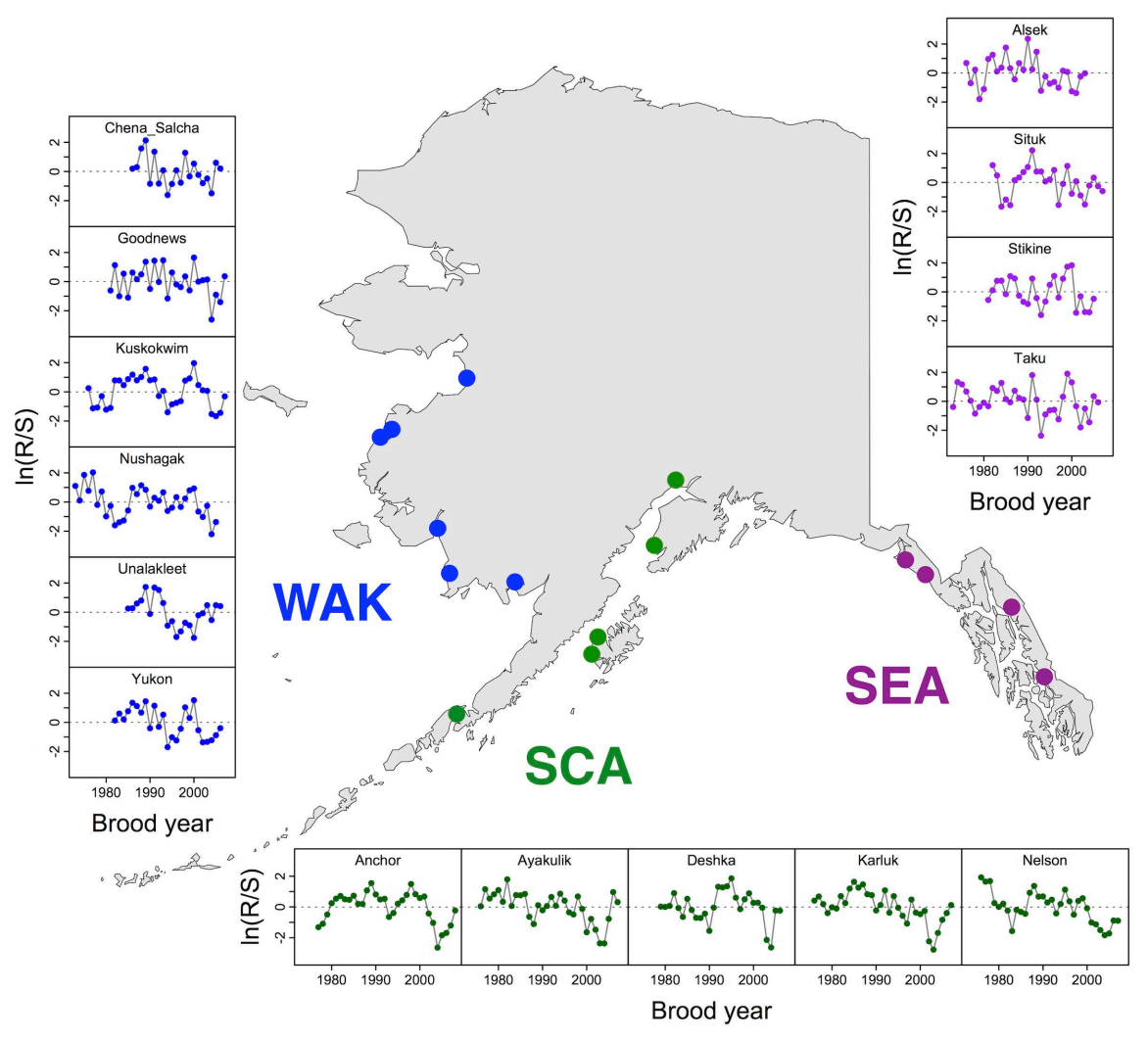
Chena_Salcha
Goodnews
Kuskokwim
Nushagak
Unalakleet
Yukon
ln(R/S)
1980 1990 2000
Brood year
Alsek
Situk
Stikine
Taku
ln(R/S)
1980 1990 2000
Brood year
WAK
SCA
SEA
Anchor
Ayakulik
Deshka
Karluk
Nelson
ln(R/S)
1980 1990 2000
Brood year

Trend

-4 -2 0 2 4

1975 1980 1985 1990 1995 2000 2005

Brood year

Trend

-4 -2 0 2 4

Loadings

-0.6 -0.2 0.2 0.6

Chena_Salcha
Goodnews
Kuskokwim
Nushagak
Unalakleet
Yukon

Anchor
Ayakulik
Deshka
Karluk
Nelson

Alsek
Situk
Stikine
Taku

Loadings

-0.6 -0.2 0.2 0.6

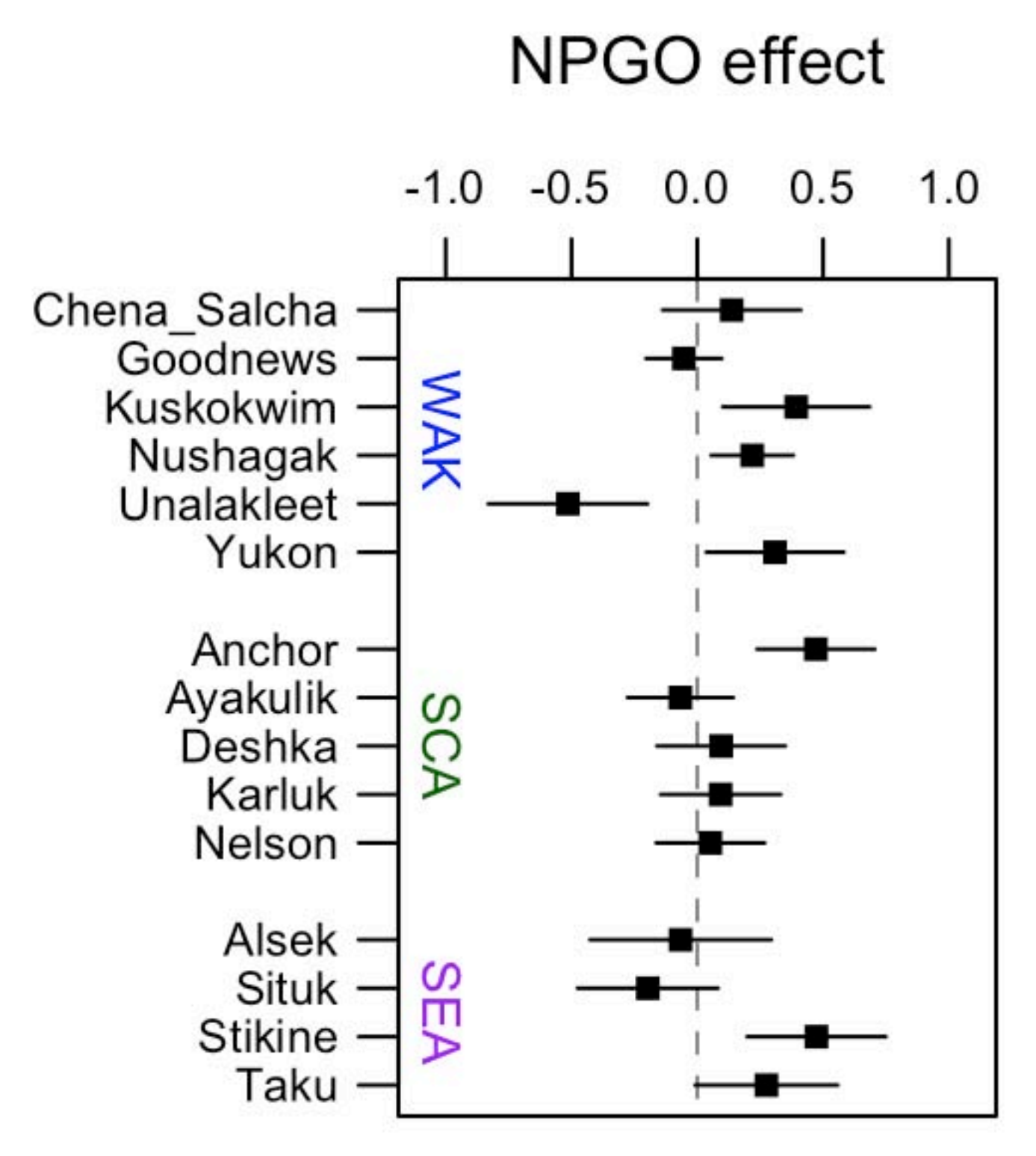
NPGO effect
-1.0
-0.5
0.0
0.5
1.0
Chena_Salcha
Goodnews
Kuskokwim
Nushagak
Unalakleet
Yukon
Anchor
Ayakulik
Deshka
Karluk
Nelson
Alsek
Situk
Stikine
Taku
WAK
SCA
SEA

WAK

SCA

SEA

Trend

Loadings

Brood year

Stocks

Chena_Salcha
Goodnews
Kuskokwim
Nushagak
Unalakleet
Yukon

Anchor
Ayakulik
Deshka
Karluk
Nelson

Alsek
Situk
Stikine
Taku

WAK
SCA
SEA
Covariate effect
ICE
RUS
NPGO
BSAI
RUS
BOG
RUS
ICE
1
0
-1
Chena_Salcha
Goodnews
Kuskokwim
Nushagak
Unalakleet
Yukon
Anchor
Ayakulik
Deshka
Karluk
Nelson
Alsek
Situk
Stikine
Taku

Chena_Salcha
Goodnews
Anchor
Kuskokwim
Ayakulik
Alsek
Nushagak
Deshka
Situk
Unalakleet
Karluk
Stikine
Yukon
Nelson
Taku
ln(R/S)
Brood year

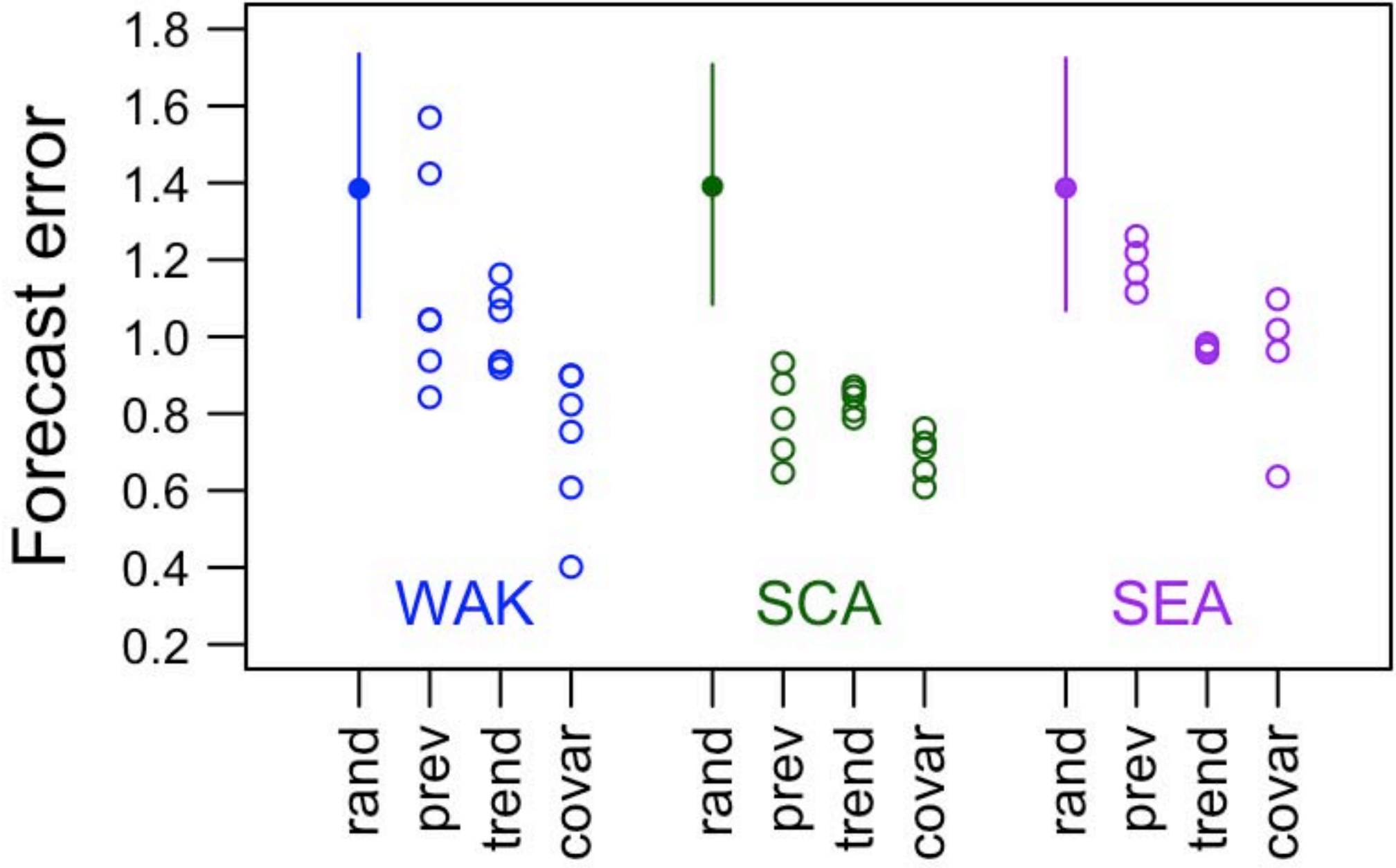
Forecast error
1.8
1.6
1.4
1.2
1.0
0.8
0.6
0.4
0.2
WAK
SCA
SEA
rand
prev
trend
covar
rand
prev
trend
covar
rand
prev
trend
covar

I. MODEL SELECTION RESULTS

List of abbreviations for indicators used in the models:

TEMP - Air temperature on land

ICE – River ice break-up

SLP - Sea level pressure

SST - Sea-surface temperature

SWI - Strong winds index

AO - Arctic Oscillation

PDO - Pacific Decadal Oscillation

NPI - North Pacific Index

NPGO - North Pacific Gyre Oscillation

BOG - Walleye pollock biomass from the Bogoslof region in the Eastern Bering Sea

BSAI – Bering Sea and Aleutian Islands Chinook bycatch

KAM - Kamchatka pink abundance

RUS - Russian Chinook catch

Numbers after the indicators in the following tables refer to the time lag in years relative to the brood year (e.g. ICE.2 refers to the timing of river ice break-up in the second spring), and lower case letters indicate the season (a-annual, w-winter, s-spring).

Table A1: Model selection results for the Alaska-wide model (AK). Given are the covariates, number of shared trends, ΔAICc values, and Akaike weights for the top 20 models.

Indicator 1	Indicator 2	Indicator 3	Trends	ΔAICc	Akaike weights
NPGO.w2	NA	NA	2	0	0.514
ICE.2	NA	NA	3	2.8	0.129
RUS.3	NA	NA	3	3.6	0.085
ICE.2	RUS.3	NA	2	4.5	0.055
RUS.3	NA	NA	2	4.9	0.044
ICE.2	RUS.3	NA	3	5.4	0.035
NA	NA	NA	3	5.7	0.029
ICE.2	BSAI.2	NA	3	5.8	0.028
NPGO.w2	ICE.2	NA	2	6	0.025
NPGO.a2	NA	NA	2	7.6	0.011
ICE.2	NA	NA	2	8	0.01
NPGO.s2	BSAI.2	NA	2	9.3	0.005
NPGO.w2	BSAI.2	NA	2	9.6	0.004
NPGO.w2	NA	NA	3	10.5	0.003
NPGO.a2	BSAI.2	NA	2	10.7	0.002
NPGO.a2	NA	NA	3	11	0.002
NPGO.w2	RUS.3	NA	3	11.1	0.002
NPGO.s2	NA	NA	2	11.1	0.002
NPGO.s2	NA	NA	3	11.7	0.001
NPGO.w2	RUS.3	NA	2	12.2	0.001

Table A2: Model selection results for Western Alaska (WAK). Given are the covariates, number of shared trends, ΔAICc values, and Akaike weights for the top 20 models.

Indicator 1	Indicator 2	Indicator 3	Trends	ΔAICc	Akaike weights
ICE.2	RUS.3	NPGO.w2	1	0	0.243
ICE.2	RUS.3	NA	1	0.71	0.171
PDO.w2	ICE.2	RUS.3	1	1.21	0.133
ICE.2	RUS.3	BSAI.2	1	1.59	0.11
ICE.2	RUS.4	NA	1	1.95	0.092
ICE.2	RUS.3	BSAI.4	1	2.23	0.08
ICE.2	RUS.4	BSAI.4	1	5.08	0.019
ICE.2	RUS.3	NPGO.a2	1	5.5	0.016
ICE.2	RUS.4	NPGO.w2	1	6.34	0.01
ICE.2	RUS.5	NPGO.w2	1	6.49	0.009
SST.w2	ICE.2	RUS.4	1	6.58	0.009
ICE.2	RUS.3	NPGO.s2	1	6.87	0.008
PDO.w2	ICE.2	RUS.4	1	6.89	0.008
ICE.2	RUS.4	BSAI.2	1	6.91	0.008
SST.w2	ICE.2	RUS.3	1	6.98	0.007
SST.s2	ICE.2	RUS.4	1	7.25	0.006
SST.s2	ICE.2	RUS.3	1	7.27	0.006
ICE.2	RUS.4	NPGO.a2	1	8.65	0.003
ICE.2	RUS.4	NPGO.s2	1	8.91	0.003
PDO.a2	ICE.2	RUS.3	1	9.42	0.002

Table A3: Model selection results for Southcentral Alaska (SCA). Given are the covariates, number of shared trends, ΔAICc values, and Akaike weights for the top 20 models.

Indicator 1	Indicator 2	Indicator 3	Trends	ΔAICc	Akaike weights
RUS.3	BSAI.2	BOG.2	1	0	0.577
RUS.5	BSAI.2	BOG.2	1	4.8	0.053
RUS.3	BSAI.2	NA	2	5.2	0.042
RUS.4	BSAI.2	BOG.2	1	6.1	0.028
BSAI.2	BOG.2	NA	2	6.3	0.025
RUS.3	BOG.2	NA	2	7.6	0.013
RUS.3	BSAI.2	NA	1	7.7	0.012
RUS.4	BSAI.2	NA	1	7.8	0.012
RUS.3	BSAI.3	BOG.2	2	8.4	0.009
BSAI.3	BOG.2	NA	3	8.5	0.008
RUS.3	BSAI.2	BOG.2	2	8.6	0.008
BSAI.2	BOG.2	NA	1	8.7	0.008
RUS.5	BSAI.2	BOG.2	2	8.8	0.007
RUS.3	NA	NA	3	9	0.007
RUS.3	BSAI.2	NPGO.s2	2	9.2	0.006
BOG.2	NA	NA	3	9.6	0.005
RUS.4	BSAI.2	NA	2	10.1	0.004
BSAI.2	BOG.2	NPGO.s2	2	10.3	0.003
SST.w2	RUS.3	BOG.2	2	10.4	0.003
RUS.3	BSAI.2	NA	3	10.6	0.003

Table A4: Model selection results for Southeast Alaska (SEA). Given are the covariates, number of shared trends, ΔAICc values, and Akaike weights for the top 20 models.

Indicator 1	Indicator 2	Indicator 3	Trends	ΔAICc	Akaike weights
RUS.3	ICE.1	NA	1	0	0.377
RUS.3	BSAI.2	ICE.1	1	0.41	0.307
RUS.3	NPGO.a2	ICE.1	1	3.69	0.06
RUS.3	NA	NA	2	4.23	0.045
PDO.a2	RUS.3	ICE.1	1	4.97	0.031
RUS.3	NPGO.w2	ICE.1	1	5.33	0.026
RUS.4	BSAI.2	ICE.1	1	6.2	0.017
RUS.3	NA	NA	1	6.52	0.014
RUS.3	BSAI.2	NA	2	6.84	0.012
RUS.5	BSAI.2	ICE.1	1	7.24	0.01
RUS.3	NPGO.a2	NA	1	7.48	0.009
RUS.4	ICE.1	NA	1	7.53	0.009
RUS.5	ICE.1	NA	1	8.18	0.006
RUS.3	ICE.1	NA	2	8.61	0.005
RUS.3	ICE.1	TEMP.1	1	8.69	0.005
PDO.a2	RUS.5	ICE.1	1	8.97	0.004
RUS.3	SST.s2	ICE.1	1	9.14	0.004
RUS.3	ICE.1	TEMP.2	1	9.2	0.004
RUS.3	SST.s2	ICE.1	1	9.42	0.003
RUS.3	BSAI.2	NA	1	9.63	0.003

Table A5: Model selection results for the alternative model of Western Alaska (WAK) including the Nelson River population. Given are the covariates, number of shared trends, ΔAICc values, and Akaike weights for the top 5 models.

Indicator 1	Indicator 2	Indicator 3	Trends	ΔAICc	Akaike weights
ICE.2	RUS.3	NA	2	0	0.274
ICE.2	RUS.3	NPGO.w2	2	0.29	0.237
ICE.2	NPGO.w2	NA	2	1.07	0.16
ICE.2	NA	NA	2	3.4	0.05
PDO.w2	ICE.2	RUS.3	2	3.83	0.04

Table A6: Model selection results for the alternative model of Southcentral Alaska (SCA) without the Nelson River population. Given are the covariates, number of shared trends, ΔAICc values, and Akaike weights for the top 5 models.

Indicator 1	Indicator 2	Indicator 3	Trends	ΔAICc	Akaike weights
RUS.3	BSAI.2	NA	1	0	0.425
RUS.3	BSAI.2	NA	2	4.1	0.054
SST.w2	RUS.3	BSAI.2	1	4.3	0.05
RUS.3	NA	NA	2	4.3	0.05
RUS.3	BSAI.2	NPGO.a2	1	4.5	0.044

II. MODEL PREDICTED VERSUS OBSERVED

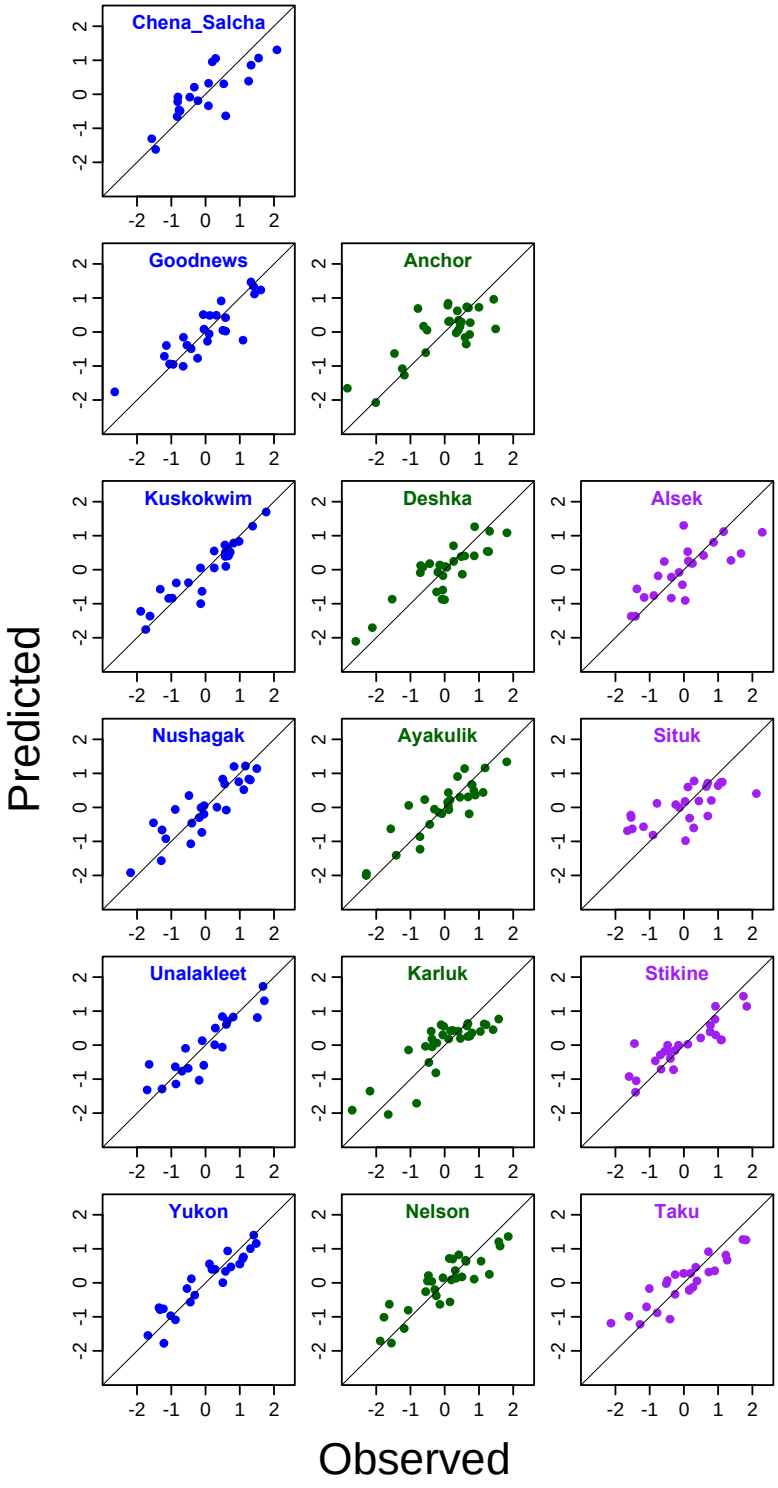

Fig. A1: Plot of predicted versus observed values of ln(R/S). Model predictions derive from the regional models as presented in figs 4-6.

III. MODELS ACCOUNTING FOR DENSITY DEPENDENCE

Table A7: Comparison of indicators and trends (m) included in the top models for the statewide (AK) and regional analyses (WAK/SCA/SEA) using either the natural logarithm of recruits per spawner or the residuals of the Ricker fit. Alternative models presented in Figs A2 and A3 are indicated in bold (note that, where possible, models with the same number of indicators were selected if the ΔAICc was smaller than 2, i.e. if there was no clear support for any one model).

	ln(R/S)		**Residuals of Ricker fit**				
	1st model	m	1st model	m	ΔAICc	2nd model	m
AK	NPGO.a2	2	**NPGO.a2 BSAI.4**	**2**	0.9	NPGO.w2 BSAI.4	2
WAK	ICE.2 RUS.3 NPGO.w2	1	**ICE.2, RUS.3, TEMP.2**	**1**	1.2	ICE.2 TEMP.2	1
SCA	RUS.3 BSAI.2 BOG.2	1	BSAI.4, NPGO.a2	2	**0.75**	**RUS.3 BSAI.4 BOG.2**	**2**
SEA	RUS.3 ICE.1	1	RUS.3	2	**0.96**	**RUS.3 SST.s2**	**2**

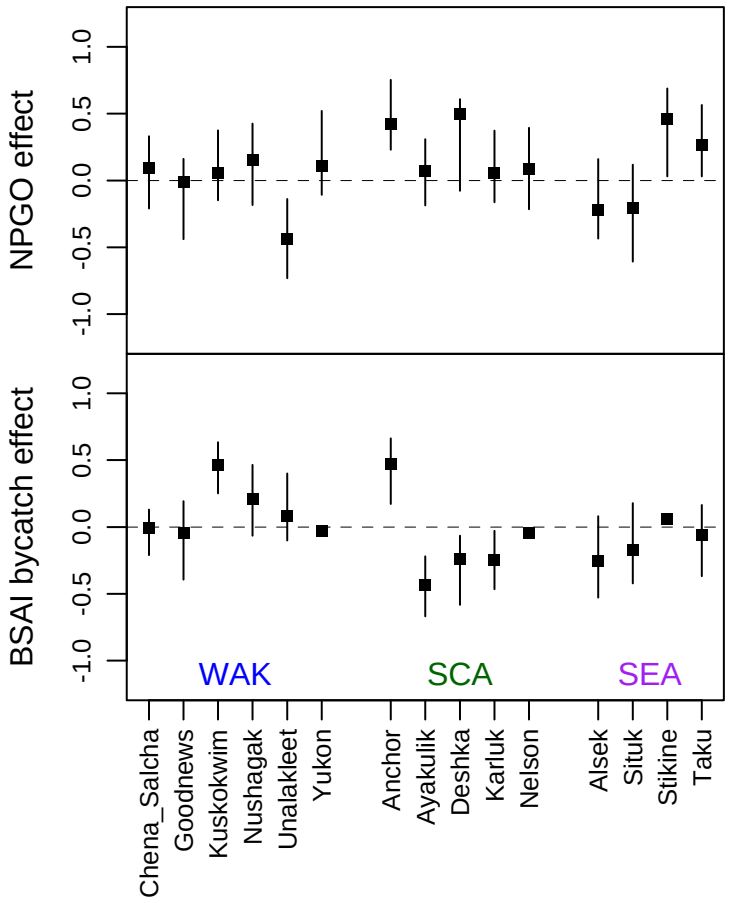

Fig. A2: **Covariate effects of the alterative statewide model as presented in Table A7.** Shown are maximum likelihood estimates and 95% confidence intervals for covariates included into the best model, as indicated in Table A7.

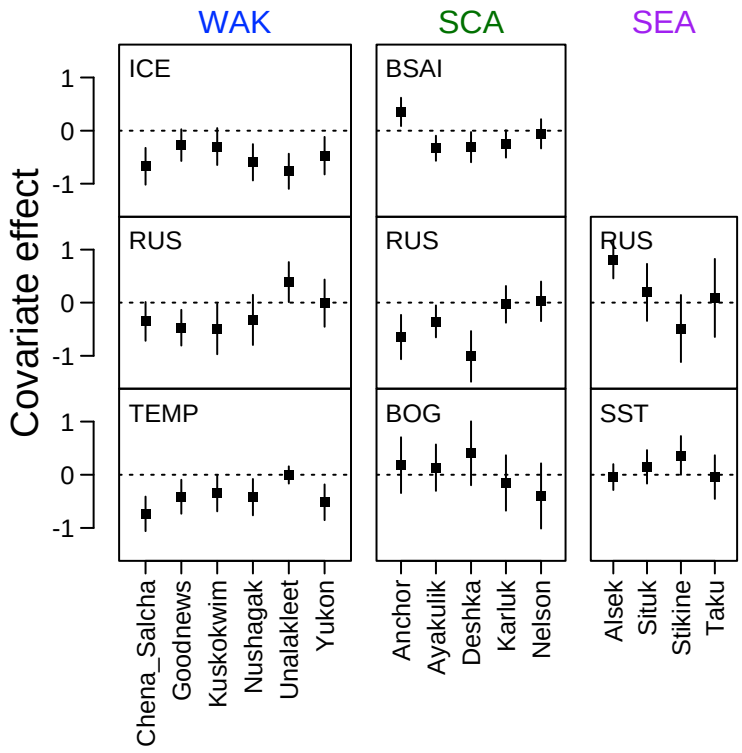

Fig. A3: **Covariate effects of the alterative regional models as presented in Table A7.** Shown are maximum likelihood estimates and 95% confidence intervals for covariates included into the best or second best (ΔAICc<2) model for each region, as indicated in Table A7 (note that models with the same number of covariates were selected if the ΔAICc was smaller than 2).